

# RECONSTRUCTION OF SURFACE OF REVOLUTION FROM MULTIPLE UNCALIBRATED VIEWS: A BUNDLE-ADJUSTMENT APPROACH

Hui Zhang<sup>†</sup>, Kwan-Yee K. Wong<sup>†</sup>, Paulo R. S. Mendonça<sup>‡</sup>

Department of Computer Science and Information Systems<sup>†</sup>  
The University of Hong Kong, Pokfulam Rd, HK

GE Global Research Center Schenectady, NY 12301, USA<sup>‡</sup>

## ABSTRACT

This paper addresses the problem of recovering the 3D shape of a surface of revolution from multiple uncalibrated perspective views. In previous work, we have exploited the invariant properties of the surface of revolution and its silhouette to recover the contour generator and hence the meridian of the surface of revolution from a single uncalibrated view. However, there exists one degree of freedom in the reconstruction which corresponds to the unknown orientation of the revolution axis of the surface of revolution. In this paper, such an ambiguity is removed by estimating the horizon, again, using the image invariants associated with the surface of revolution. A bundle-adjustment approach is then proposed to provide an optimal estimate of the meridian when multiple uncalibrated views of the same surface of revolution are available. Experimental results on real images are presented, which demonstrate the feasibility of the approach.

## 1. INTRODUCTION

Most of the existing techniques for the reconstruction of surface of revolutions (or Straight Homogeneous Generalized Cylinders, SHGCs) follows [1] and [2], which provides algorithms for identifying the axis and the ending cross-sections of SHGC, respectively. Such techniques have been developed mainly for the case of single uncalibrated views [3] [4]. In [5], we proposed an algorithm which makes use of the invariant properties of a surface of revolution to calibrate the camera and recover its 3D shape. However, the ambiguity in the orientation of the revolution axis cannot be correctly resolved. Besides, the problems of how to obtain an optimal solution for the camera calibration and the final reconstruction in the case of multiple views and the problem of self-occlusion has not been handled.

This paper addresses the problem of recovering the 3D shape of a surface of revolution from multiple uncalibrated perspective views. In this paper, we exploit the invariant properties of the surface of revolution and its silhouettes

to locate both the imaged revolution axis and the vanishing line(horizon) of the cross sections. These are used to calibrate the intrinsic parameters of the cameras[6], rectify the images such that each resultant silhouette exhibits bilateral symmetry. The ambiguity in the orientation of the revolution axis is removed during rectification with the information provided by the horizon. The contour generators, and hence the meridians, can then be recovered from each image. To find optimal estimates for the meridian and the camera parameters, a base meridian is first computed from meridians computed from all views. Bundle-adjustment, an approach refining a visual reconstruction to produce jointly optimal 3D structure and viewing parameter estimates [7] [8], is then employed to refine the camera parameters, rectification homographies and the shape information of the meridian. This work is different from previous work in that, rather than optimizing points, bundle adjustment is, for the first time, applied to curves and meridians. The problem of self-occlusion is also "resolved" with the availability of multiple views.

This paper is organized as follows. Section 2 presents the theoretical background and our novel approach for reconstructing a surface of revolution from a single uncalibrated image. Section 3 presents the optimal meridian estimation and the bundle-adjustment method for reconstruction of a surface of revolution from multiple views. Results of real data experiments are presented in Section 4 and conclusions are given in Section 5.

## 2. RECONSTRUCTION FROM A SINGLE VIEW

### 2.1. Invariant Properties of a surface of revolution

**Harmonic Homology** Under perspective projection, the image of a surface of revolution will be invariant to a *harmonic homology* [9][10]

$$\mathbf{W} = \mathbf{I}_3 - 2 \frac{\mathbf{v}_x \mathbf{l}_s^T}{\mathbf{v}_x^T \mathbf{l}_s}, \quad (1)$$

where  $\mathbf{l}_s$  is the imaged revolution axis, and  $\mathbf{v}_x$  is the vanishing point associated with normal of the plane containing the revolution axis and the camera center. If the camera is pointing towards the revolution axis,  $\mathbf{W}$  will reduce to a skew symmetry  $\mathbf{S}$  where  $\mathbf{v}_x$  is at infinity. If the camera also has unit aspect ratio,  $\mathbf{S}$  will become a bilateral symmetry  $\mathbf{T}$  where  $\mathbf{v}_x$  is both at infinity and having a direction orthogonal to  $\mathbf{l}_s$ .

**Planar Homology** A plane projective transformation  $\mathbf{U}$  is a planar homology if it has a line  $\mathbf{l}_f$  of fixed points together with a fixed point  $\mathbf{v}_w$  [11]. The planar homology can be defined by

$$\mathbf{U} = \mathbf{I}_3 + (\mu - 1) \frac{\mathbf{v}_w \mathbf{l}_f^T}{\mathbf{v}_w^T \mathbf{l}_f}, \quad (2)$$

where the line  $\mathbf{l}_f$  is called the axis, and the fixed point  $\mathbf{v}_w$  is called the vertex. The cross ratio  $\mu$  defined by the vertex, a pair of corresponding points, and the intersection of the corresponding line with the fixed axis, is invariant for all points related by the homology. The harmonic homology is the special case of a planar homology where its invariant cross ratio is  $-1$ .

In the case of a surface of revolution, the planar homology  $\mathbf{U}$  arises in the images  $\mathbf{C}_1$  and  $\mathbf{C}_2$  of two cross sections of the surface of revolution (see Fig. 1(b)). The vertex  $\mathbf{v}_w$  is given by the intersection of the bitangent lines of the conics  $\mathbf{C}_1$  and  $\mathbf{C}_2$ , the axis  $\mathbf{l}_f$  is the horizon of the planes where the cross sections of the surface of revolution lie on.

The axis  $\mathbf{l}_f$  and the vertex  $\mathbf{v}_w$  of the planar homology  $\mathbf{U}$ , and axis  $\mathbf{l}_s$  of the harmonic homology  $\mathbf{W}$  are the image invariants to be exploited to calibrate the camera and rectify the images.

## 2.2. Invariants Estimation

This section introduces a novel approach to obtain the image invariants of a surface of revolution which are the vanishing point  $\mathbf{v}_x$ , the imaged revolution axis  $\mathbf{l}_s$  and the horizon  $\mathbf{l}_f$ . Given the silhouette of a surface of revolution, two conics  $\mathbf{C}_1$  and  $\mathbf{C}_2$  can be fitted to two imaged cross sections of the surface of revolution. Let the external bitangent points at  $\mathbf{C}_1$  and  $\mathbf{C}_2$  be  $\mathbf{x}_1, \mathbf{x}'_1$  and  $\mathbf{x}_2, \mathbf{x}'_2$ , respectively (see Fig. 1(a)). As  $\mathbf{x}_1, \mathbf{x}_2$  and  $\mathbf{x}'_1, \mathbf{x}'_2$  are related by the harmonic homology  $\mathbf{W}$  as introduced in section 2.1, the vertex  $\mathbf{v}_x$  and the axis  $\mathbf{l}_s$  of  $\mathbf{W}$  can be easily obtained by

$$\mathbf{v}_x = (\mathbf{x}_1 \times \mathbf{x}_2) \times (\mathbf{x}'_1 \times \mathbf{x}'_2) \quad (3)$$

$$\mathbf{l}_s = ((\mathbf{x}_1 \times \mathbf{x}'_1) \times (\mathbf{x}_2 \times \mathbf{x}'_2)) \times ((\mathbf{x}_1 \times \mathbf{x}'_2) \times (\mathbf{x}_2 \times \mathbf{x}'_1)). \quad (4)$$

The  $\mathbf{v}_x$  and  $\mathbf{l}_s$  will be refined by making use of the whole silhouette with equation (21) in section 3.2.

The two conics and their external bitangent lines forms a perspective projection of a virtual cone in 3D space, where

the two conics corresponds to two cross sections and the bitangent lines corresponds to two meridians of the cone. Four parallel planes can be assumed existing in 3D which correspond to the vertex  $\mathbf{v}_x$ , the two conics  $\mathbf{C}_1, \mathbf{C}_2$  and the horizon. After perspective projection, the cross ratio  $\mu$  formed by the intersection of any line with these four planes in 3D will be invariant. For the planar homology  $\mathbf{U}$ , let points  $\mathbf{w}_1, \mathbf{w}_2$  be the intersection between the horizon  $\mathbf{l}_f$  and the line joining  $\mathbf{x}_1$  and  $\mathbf{x}'_1$ ,  $\mathbf{l}_f$  and the line joining  $\mathbf{x}_2$  and  $\mathbf{x}'_2$ , respectively (see Fig. 1(b)). Thus the cross ratio  $\{\mathbf{v}_w, \mathbf{x}_1, \mathbf{x}'_1, \mathbf{w}_1\}$  is equal to  $\{\mathbf{v}_w, \mathbf{x}_2, \mathbf{x}'_2, \mathbf{w}_2\}$ .

Generally, the plane formed by the camera center and the revolution axis cuts the virtual cone at two meridians. These two meridians intersect with conics  $\mathbf{C}_1$  and  $\mathbf{C}_2$  at  $\mathbf{x}_3, \mathbf{x}'_3$  and  $\mathbf{x}_4, \mathbf{x}'_4$ , respectively. Let  $\mathbf{w}$  be the intersection between the imaged revolution axis  $\mathbf{l}_s$  and horizon  $\mathbf{l}_f$ . Note that the intersection point  $\mathbf{w}$  is also the vanishing point  $\mathbf{v}_z$  of  $z$ -axis. Because of the invariant property of the cross ratio,  $\{\mathbf{v}_w, \mathbf{x}_3, \mathbf{x}'_3, \mathbf{v}_z\}$  is equal to  $\{\mathbf{v}_w, \mathbf{x}_4, \mathbf{x}'_4, \mathbf{v}_z\}$ , which is also equal to  $\{\mathbf{v}_w, \mathbf{x}_1, \mathbf{x}'_1, \mathbf{w}_1\}$  and  $\{\mathbf{v}_w, \mathbf{x}_2, \mathbf{x}'_2, \mathbf{w}_2\}$ . Two constraints can be obtained

$$\{\mathbf{v}_w, \mathbf{x}_4, \mathbf{x}'_4, \mathbf{w}\} = \{\mathbf{v}_w, \mathbf{x}_3, \mathbf{x}'_3, \mathbf{w}\} \quad (5)$$

$$\{\mathbf{v}_w, \mathbf{x}'_4, \mathbf{x}_4, \mathbf{w}\} = \{\mathbf{v}_w, \mathbf{x}'_3, \mathbf{x}_3, \mathbf{w}\}, \quad (6)$$

to uniquely define  $\mathbf{w}$ . Thus the horizon  $\mathbf{l}_f$  of the horizontal planes can be computed as the cross product of the two vanishing points  $\mathbf{v}_x$  and  $\mathbf{v}_z$ , by

$$\mathbf{l}_f = \mathbf{v}_x \times \mathbf{v}_z. \quad (7)$$

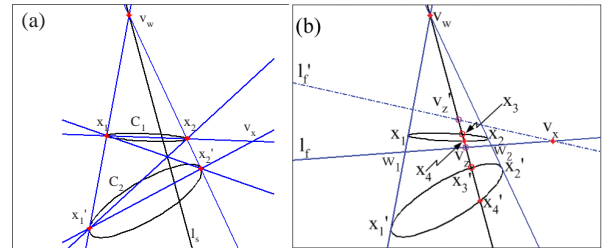


**Fig. 1.** (a) The geometric construction of the imaged revolution axis  $\mathbf{l}_s$  and the vanishing point  $\mathbf{v}_x$ . (b) The geometric construction of the horizon.

Note an additional situation exists where  $\mathbf{x}_3$  and  $\mathbf{x}_4$  are mapped to  $\mathbf{x}'_4, \mathbf{x}'_3$  rather than  $\mathbf{x}'_3, \mathbf{x}'_4$  as described above, which will give an ambiguity in choosing vanishing point of  $z$ -axis and thus the vanishing line ( $\mathbf{v}'_z$  and  $\mathbf{l}'_f$  in Fig. 1(b)). Yet this ambiguity can be resolved by the visibility of the imaged cross section.

### 2.3. Camera calibration

Under general perspective projection, the image of a surface of revolution will be invariant to a harmonic homology  $\mathbf{W}$ . Its vertex  $\mathbf{v}_x$  and axis  $\mathbf{l}_s$  are related by the pole-polar relationship [6]

$$\omega \mathbf{v}_x = \mathbf{l}_s, \quad (8)$$

where  $\omega = \mathbf{K}^{-T} \mathbf{K}^{-1}$  is the image of the absolute conic (IAC) and  $\mathbf{K}$  is the camera calibration matrix. By assuming the skew of the camera to be zero, the matrix elements of the IAC will become

$$\omega = \begin{bmatrix} \omega_1 & 0 & \omega_2 \\ 0 & \omega_3 & \omega_4 \\ \omega_2 & \omega_4 & \omega_5 \end{bmatrix}. \quad (9)$$

The camera can be calibrated by estimating  $\omega$ . Let  $\mathbf{v}_x = [v_1 \ v_2 \ v_3]^T$  and  $\mathbf{l}_s = [l_1 \ l_2 \ l_3]^T$ , each pair of  $\mathbf{v}_x$  and  $\mathbf{l}_s$  provides the following two constraints [6]

$$v_1 l_3 \omega_1 + (v_3 l_3 - v_1 l_1) \omega_2 - v_2 l_1 \omega_4 - v_3 l_1 \omega_5 = 0 \quad (10)$$

$$v_1 l_2 \omega_2 - v_2 l_3 \omega_3 + (v_2 l_2 - v_3 l_3) \omega_4 - v_3 l_2 \omega_5 = 0 \quad (11)$$

Hence  $\omega$  can be estimated, up to a scale factor, by a linear least squares method given two or more pairs of  $\mathbf{v}_x$  and  $\mathbf{l}_s$ . The calibration matrix  $\mathbf{K}$  can then be obtained from  $\omega$  by Cholesky decomposition [12].

### 2.4. Image Rectification

In [5], the image of the surface of revolution is rectified by a planar homography induced by a rotation such that the resultant silhouette is bilaterally symmetric about the  $y$ -axis. Such a rotation rotates the camera about its optical center until the revolution axis of the surface of revolution lies on the  $y$ - $z$  plane at the camera coordinate system, and simplified the reconstruction of the surface of revolution (see [5] for details). However, the unknown orientation of the revolution axis on the  $y$ - $z$  plane induces one degree of freedom ambiguity in the reconstruction.

In this paper, such an ambiguity is removed by using the information provided by the estimated horizon. A planar homography  $\mathbf{H}_x$  induced by a rotation about the  $x$ -axis is computed such that the principle point lies on the transformed horizon. This corresponds to rotating the camera about its  $x$ -axis until its  $z$ -axis aligns with the  $z$ -axis of the world coordinate system. After the rectification, the configuration is now simplified to one in which the surface of revolution has its revolution axis coincides with the  $y$ -axis of the world coordinate system with an aligned pinhole camera placed along the  $z$ -axis (see Fig.2).

### 2.5. Reconstruction

Let's consider a surface of revolution  $\tilde{\mathbf{S}}_r(s, \theta)$ .  $\tilde{\mathbf{S}}_r(s, \theta) = [X(s) \cos \theta \ Y(s) \ X(s) \sin \theta]^T$  is generated by rotating a

meridian curve  $\tilde{\mathbf{C}}_r = [X(s) \ Y(s) \ 0]^T$  about the  $y$ -axis and a pinhole camera  $\hat{\mathbf{P}} = [\mathbf{I}_3 \ -\mathbf{c}]$  centered at  $\mathbf{c} = [0 \ 0 \ -d_z]^T$ , with  $d_z > 0$  (see Fig.2).

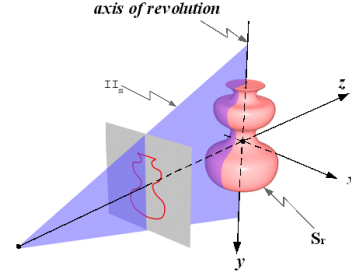


**Fig. 2.** A surface of revolution  $\mathbf{S}_r$ , whose axis of revolution coincides with the  $y$ -axis, being viewed by a pinhole camera  $\hat{\mathbf{P}} = [\mathbf{I}_3 \ -\mathbf{c}]$  centered at  $\mathbf{c} = [0 \ 0 \ -d_z]^T$ .

The contour generator can be parameterized by  $s$  as [5]

$$\Gamma(s) = \mathbf{c} + \lambda(s) \mathbf{p}(s), \quad \text{where} \quad (12)$$

$$\mathbf{p}(s) \cdot \mathbf{n}(s) = 0, \quad (13)$$

where  $\mathbf{c}$  indicates the camera center,  $\mathbf{p}(s) = [x(s) \ y(s) \ 1]^T$  is the viewing vector from  $\mathbf{c}$  to the focal plane at unit distance for the point  $\Gamma(s)$ , and  $\lambda(s)$  is the depth of  $\Gamma(s)$  from  $\mathbf{c}$  along the  $z$  direction.  $\mathbf{n}(s)$  is the unit surface normal at  $\Gamma(s)$  which can be determined as the cross product between  $\mathbf{p}(s)$  and the tangent along silhouette at  $\mathbf{p}(s)$  [5].

It can be shown that the surface normal at point  $\tilde{\mathbf{S}}_r(s_0, \theta_0)$  is normal to the meridian curve through  $\tilde{\mathbf{S}}_r(s_0, \theta_0)$  and lies on the plane containing the  $y$ -axis and the point  $\tilde{\mathbf{S}}_r(s_0, \theta_0)$ . This coplanarity constraint, expressed by [5]

$$\mathbf{n}(s)^T [\mathbf{n}_y]_{\times} \tilde{\Gamma}(s) = 0, \quad (14)$$

where  $\mathbf{n}_y = [0 \ 1 \ 0]^T$ , can be expanded to recover the depth

$$\lambda(s) = \frac{d_z n_1(s)}{n_1(s) - n_3(s)x(s)}, \quad (15)$$

and the contour generator can then be recovered using Eqn.(12).

Such reconstruction is determined up to a similarity transformation since the distance  $d_z$  cannot be recovered. The meridian which forms the surface of revolution can be obtained by

$$\tilde{\mathbf{C}}_r(s) = \begin{bmatrix} \sqrt{(\lambda(s)x(s))^2 + (\lambda(s) - d_z)^2} \\ \lambda(s)y(s) \\ 0 \end{bmatrix}. \quad (16)$$

## 3. RECONSTRUCTION FROM MULTIPLE VIEWS

### 3.1. Estimation of the Base Meridian

By using the method described in section 2.5, a meridian can be obtained from each image. However, these merid-

ians may not agree with each other due to the presence of noise and self-occlusion. A unique meridian is needed to represent the reconstructed surface of revolution from all views and here a B-spline is fitted to the meridians to provide a base meridian. The B-spline can be written as a linear combination of spline segments by

$$B(t) = \sum_{i=-k}^g c_i N_{i,k+1}(t), \quad (17)$$

where  $k$  is the degree of B-spline,  $g$  is the number of segments, and  $c_i$  are the *B-spline coefficients* (i.e., the control points).  $N_{i,k+1}(t)$  are the base functions defined by the recursive function

$$\begin{aligned} N_{i,l+1}(t) &= \frac{t-u_i}{u_{i+l}-u_i} N_{i,l}(t) + \frac{u_{i+l+1}-t}{u_{i+l+1}-u_{i+l}} N_{i+1,l}(t) \\ N_{i,1}(t) &= \begin{cases} 1 & \text{if } t \in [u_i, u_{i+1}) \\ 0 & \text{if } t \notin [u_i, u_{i+1}) \end{cases}. \end{aligned} \quad (18)$$

where  $\{u_0, \dots, u_g\}$  is the knot sequence of the B-spline. Hence to find the optimal estimate of the base meridian by spline, the problem turns to find the control points, the number and position of the knots given the meridian points. Here all the meridian points are treated independently and the optimal B-spline can therefore be found by standard curve fitting method.

Let  $(x_r, y_r)$  be the  $L$  sample points on the meridians with  $x_r < x_{r+1}$ ,  $r = 1, \dots, L$ . Consider representing the base meridian with a smooth B-spline determined by the smoothing constraint [13]

$$\sum_{r=1}^Z (w_r((x_r, y_r) - B_3(s)))^2 \leq S, \quad (19)$$

which minimizes the distances from the sampling points to the fitted B-spline whose smoothness is kept by the inequality. This can be solved by the Lagrange least squares method.  $w_r((x_r, y_r) - B_3(s))$  is the weighted distance from the sampling points to the fitted B-spline, where  $w_r$  are the weights corresponding to the sampling points,  $B_3(s)$  are the fitted cubic B-spline and  $S$  is the smoothing parameter. Non-uniform B-spline is used here for B-spline representation because generally B-splines may need more knots and control points at positions with greater curvature. The strategies in [13] have been used here to automatically place the knots within the iteration of B-spline fitting.

In addition to the smoothing constraint, other constraints on end point derivative and convexity can be used to refine the spline. Detailed explanation can be found in [13] for estimating the B-spline with these constraints.

Note that the meridians reconstructed from all views are expressed in different camera coordinates, thus it is important to scale ( $m_j$ ) and translate ( $d_{yj}$ ) the meridians along the  $y$ -axis so that they are aligned before estimating the base meridian.

### 3.2. Bundle-Adjustment

In the presence of noises, any of the camera intrinsics, homographies and the base meridian cannot be assumed to be exactly correct, a bundle-adjustment optimization is therefore needed to provide further refinement.

The parameters which can be fed into the final bundle-adjustment procedure are, the camera matrix  $\mathbf{K}$ , the rotation for each view in Sec.2.4, the scalars  $m_j$  and translations  $d_{yj}$  and B-spline control points  $c_i$ , and the number and position of knots  $\{u_0, \dots, u_g\}$  in Sec.3.1.

Given an initial estimate of the surface of revolution generated by the base meridian, the cost function can be formulated as the reprojection error of points on the surface of revolution, i.e.,

$$cost = \sum_{j=1}^X \sum_{i=1}^Y dist(\mathbf{P}_j \tilde{\Gamma}_j(s), \rho_j)^2, \quad (20)$$

where  $\tilde{\Gamma}_j(s)$  are the 3D points on the contour generator of the surface of revolution,  $\mathbf{P}_j = m_j \mathbf{K} [\mathbf{R}_j \mathbf{t}_j]$  are the projection matrix where  $\mathbf{R}_j = (\mathbf{R}_{fj} \mathbf{R}_{bj} \mathbf{R}_{aj})^{-1}$  and  $\mathbf{t}_j = [0 \ d_{yj} \ d_{z0}]^T$ , where  $d_{z0}$  is a predefined value for  $d_z$ ,  $\mathbf{R}_{fj}$  is the rotation matrix related to the rectifying homography  $\mathbf{H}_x$  defined in section 2.4, and  $\mathbf{R}_{bj}$  and  $\mathbf{R}_{aj}$  are the two rotation matrix defined in [5].

The bundle-adjustment proceeds as follows,

**i)** For each image, extract the silhouette  $\rho_i$  of surface of revolution from its image by applying Canny edge detector [14]. Fit two conics to find the top and bottom cross sections of the surface of revolution and then obtain the image invariants by the approach proposed in Section 2.1. Estimate the harmonic homology  $\mathbf{W}$  by sampling  $Q$  evenly spaced points  $\mathbf{x}_i$  along  $\rho_j$  and minimizing the orthogonal distance from the transformed sample points  $\mathbf{x}'_i = \mathbf{W}(\mathbf{v}_x, \mathbf{l}_s) \mathbf{x}_i$  to the original silhouette  $\rho_j$  [6]

$$Cost(\mathbf{v}_x, \mathbf{l}_s) = \sum_{i=1}^Q dist(\mathbf{W}(\mathbf{v}_x, \mathbf{l}_s) \mathbf{x}_i, \rho_j)^2. \quad (21)$$

**ii)** Given two or more silhouettes and the harmonic homologies, find the camera intrinsics by estimating the image of the absolute conics  $\omega$  using equation (10) and (11).

**iii)** For each image, compute a planar homography  $\mathbf{H}'_r = \mathbf{H}_x \mathbf{H}_r$  to rectify the image such that the resultant silhouette exhibit bilateral symmetry.  $\mathbf{H}_r$  is the rectifying homography defined in [5].

**iv)** Recover the meridians with (12). Normalize and align them to get the scalars  $m_j$  and translators  $d_{yj}$ . Estimate the optimal base meridian with the constraint in (19).

**v)** Feed the parameters estimated from the previous steps to (20) to minimize the reprojection errors of the surface of

revolution. This can be solved by the Levenberg-Marquardt method [12].

With these steps, the bundle-adjustment will refine all the estimated motion and shape parameters, especially the ambiguity in the orientation of  $y$ -axis and the control points of the B-spline representing the base meridian.

#### 4. EXPERIMENTS AND RESULTS

Experiments are carried out to demonstrate the feasibility of our novel approach for reconstruction of surface of revolution from multiple views. We first present the problems existing in reconstruction from a single view with the approach of [5](see Fig.3). The left column of Fig.3(c) shows self-occlusion of a candle holder where the contour generator does not intersect a subset of the cross sections. Due to self-occlusion, middle part of the candle holder cannot be correctly reconstructed. The right column of Fig.3(d) shows with the single ellipse fitting approach in [5], the ambiguity in the orientation of the revolution axis cannot be correctly recovered. The upper and lower parts of the candle holder turn bend due to the bad estimate of the orientation.

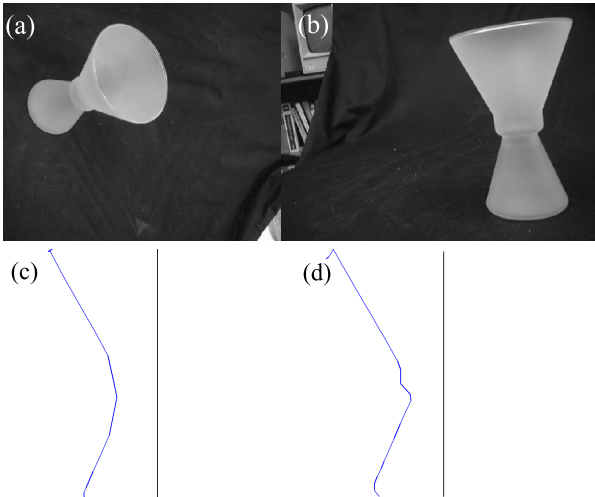


**Fig. 3.** (a) Image of a candle holder with self-occlusion. (b) A general view of the candle holder in (a). (c) Meridian reconstructed from the view in (a). (d) Meridian reconstructed with a wrong estimate of  $\phi_0$  from the view in (b).

Fig.4 shows the reconstruction of the candle holder, where the problems of self-occlusion and the ambiguity in the orientation of the revolution axis are both resolved using our algorithm. The silhouette of each image exhibits bilateral symmetry after rectification (see Fig.4(c)). The invariant cross ratio facilitates the detection of the horizon which helps to remove the ambiguity in the orientation of the revolution axis(see Fig.4(d)). A B-spline is used to represent the base meridian

(see Fig.4(e)), generating the 3D shape of the candle holder (Fig.4(f)). In implementation, only the position of the control points are optimized because, after the curve fitting, the number and position of the knots are relatively fixed, and only the control points will have great effect on the shape of the base meridian.

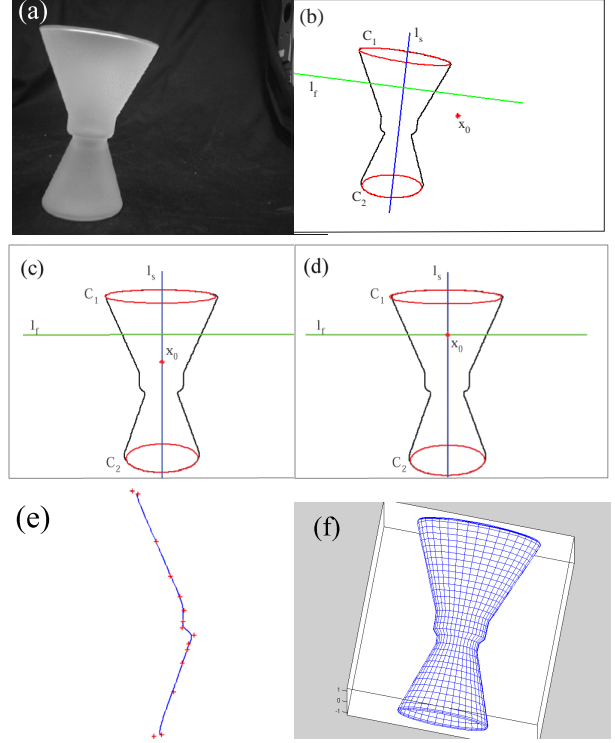


**Fig. 4.** (a) A image in a sequence of a candle holder. (b) Canny edge extracted from the image in (a), together with two fitted conics and image invariants. (c) Rectified silhouette and invariants of (b) which exhibits bilateral symmetry. (d) Rectified silhouette and invariants of (c) where intersection between  $l_s$  and  $l_f$  coincides with the principle point. (e) Reconstructed base meridian with the smoothing B-spline fitting. (f) Reconstructed model with bundle-adjustment, generated by rotating the refined base meridian around the axis of revolution.

**Table 1.** Reconstruction of a candle holder compared between results from single view with from multiple views.

Results	View 1	View 2	View 3	View 4	All Views
Ratio	0.3209	0.3036	0.3142	0.3198	0.3360
Relative error	3.72%	8.93%	5.75%	4.05%	0.81%

The reconstruction of the candle holder has been refined compared with [5]. The radius of the topmost circle and the height, measured manually using a ruler with a resolution of 1 mm, are 5.7 cm and 17.1 cm respectively. The ground truth value for the ratio of these two values of the reconstructed candle holder is 0.3333 (5.7/17.1). The im-

provement in precision can be seen from Table 1, where row 2 gives out the ratio of the topmost circle to the height of the reconstructed candle holder from 4 single images and from all images, row 3 shows the error of the ratio relative to the ground truth value. Another example is given in Fig. 5, which shows the reconstruction of a bowl. The radius of the topmost circle and the height of the bowl were 6.4 cm and 6.2 cm respectively. The ground truth value for the ratio of these two values of the reconstructed bowl is 1.0323 (6.4/6.2). The improvement in precision can be seen from Table 2. The reconstruction from all images has the minimum relative error, and this proves the feasibility of our bundle-adjustment algorithm.

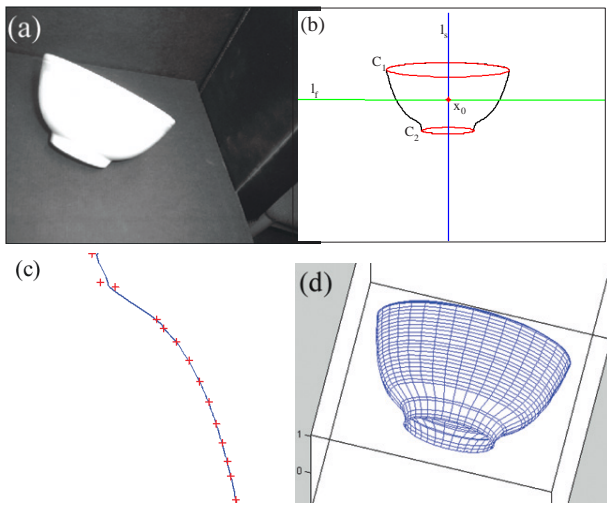


**Fig. 5.** (a) A image in a sequence of a bowl. (b) Rectified silhouette and invariants of (c) where intersection between  $l_s$  and  $l_f$  coincides with the principle point. (c) Reconstructed base meridian with the smoothing B-spline fitting. (d) Reconstructed model with bundle-adjustment, generated by rotating the refined base meridian around the axis of revolution.

**Table 2.** Reconstruction of a bowl compared results from single view with that from multiple views.

Results	View 1	View 2	View 3	View 4	All Views
Ratio	0.9610	0.9773	0.9514	0.9392	1.0474
Relative error	7.13%	5.49%	8.06%	9.30%	1.46%

## 5. CONCLUSIONS

In this paper, a novel approach is proposed to obtain the image invariants of a surface of revolution and to reconstruct it from a single uncalibrated view. By exploiting information containing in all views, a bundle-adjustment technique is also developed to remove the problems existing in reconstruction from a single view. The ambiguity in the orientation of the revolution axis is naturally removed by image

rectification. The meridians reconstructed from all views have been used for computing a base meridian by fitting with a smooth B-spline. The base meridian and the camera parameters are then refined with a bundle adjustment process by minimizing the reprojection errors. The algorithm attains an optimal reconstruction by simultaneously refining the camera intrinsics, rectifying homographies and the shape of the meridian.

**Acknowledgements** This project is partially supported by a grant from the University of Hong Kong.

## 6. REFERENCES

- [1] J. Ponce, D. Chelberg, and W. B. Mann, "Invariant properties of straight homogeneous generalized cylinders and their contours," *IEEE Trans. on Pattern Analysis and Machine Intelligence*, vol. 11, pp. 951–966, 1989.
- [2] H. Sato and T. O. Binford, "On finding the ends of shgcs in an edge image," *Image Understanding Workshop*, pp. 379–388, 1992.
- [3] Bimbo A. D. Colombo, C. and F. Pernici, "Uncalibrated 3d metric reconstruction and flattened texture acquisition from a single view of a surface of revolution," *1st International Symposium on 3D Data Processing Visualization and Transmission (3DPVT'02)*, June 2002.
- [4] S. Utcke and A. Zisserman, "Projective reconstruction of surfaces of revolution," in *DAGM03*, pp. 265–272.
- [5] K.-Y. K. Wong, P. R. S. Mendonça, and R. Cipolla, "Reconstruction of surfaces of revolution from single uncalibrated views," *Proc. British Machine Vision Conference 2002*, vol. 1, pp. 93–102, September 2002.
- [6] K.-Y. K. Wong, P. R. S. Mendonça, and R. Cipolla, "Camera calibration from surfaces of revolution," *IEEE Trans. on Pattern Analysis and Machine Intelligence*, vol. 25(2), pp. 147–161, February 2003.
- [7] B. Triggs, P. McLauchlan, R. Hartley, and A. Fitzgibbon, "Bundle adjustment – A modern synthesis," in *Vision Algorithms: Theory and Practice*, W. Triggs, A. Zisserman, and R. Szeliski, Eds., LNCS, pp. 298–375. Springer Verlag, 2000.
- [8] P. Fua, "Regularized bundle-adjustment to model heads from image sequences without calibration data," vol. 38(2), pp. 153–171, 2000.
- [9] P. R. S. Mendonça, K.-Y. K. Wong, and R. Cipolla, "Epipolar geometry from profiles under circular motion," *IEEE Trans. on Pattern Analysis and Machine Intelligence*, vol. 23(6), pp. 604–616, June 2001.
- [10] H. S. M. Coxeter, *Introduction to Geometry*, Wiley and Sons, New York, January 1989.
- [11] R. I. Hartley and A. Zisserman, *Multiple View Geometry in Computer Vision*, Cambridge University Press, Cambridge, UK, 2000.
- [12] W. H. Press, S. A. Teukolsky, W. T. Vetterling, and B. P. Flannery, *Numerical Recipes in C : The Art of Scientific Computing*, Cambridge University Press, Cambridge, UK, January 1993.
- [13] P. Dierckx, *Curve and Surface Fitting with Splines*, LNCS. Oxford Science Publications, 1993.
- [14] J. Canny, "A computational approach to edge detection," vol. 8(6), pp. 679–698, November 1986.